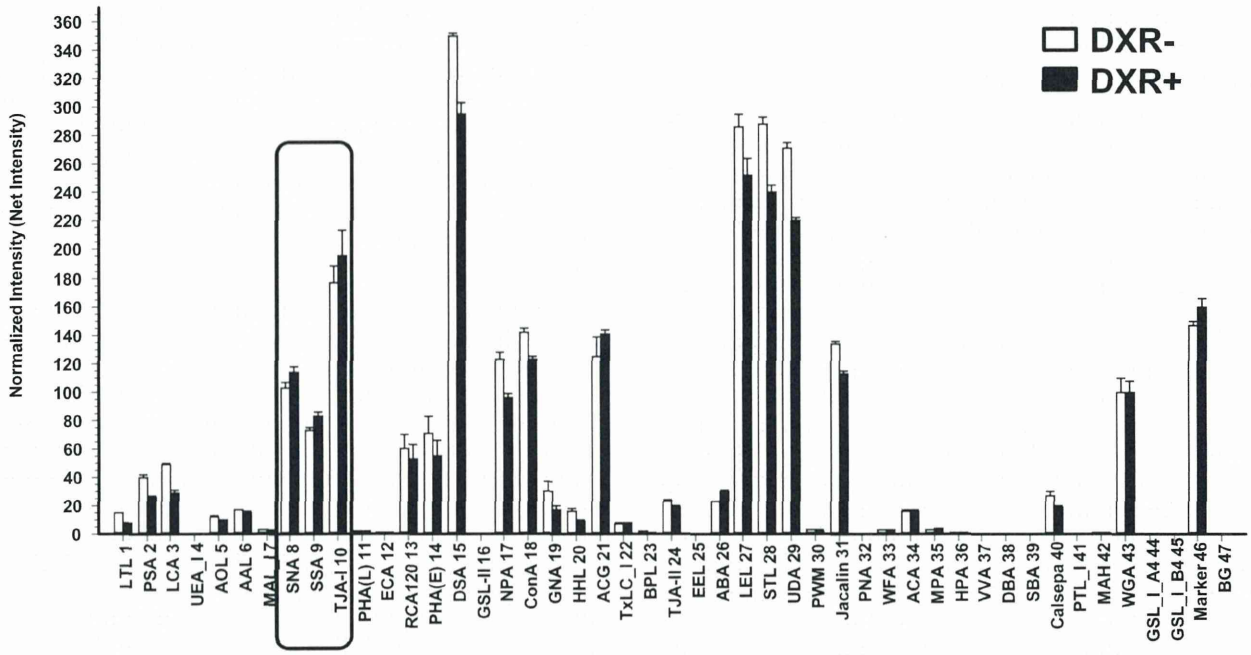

Figure 1. Lectin microarray analysis. Total cellular proteins of Huh7 cells treated with or without doxorubicin were analyzed three times using lectin microarray. Twenty-five nanogram aliquots of Cy3-labeled proteins were applied to each lectin microarray. The fluorescence intensity of each lectin was normalized to the intensity of WGA staining. All data are represented as mean ± standard deviations (SD). The Wilcoxon test was used to assess any significant differences in variables. There were significant increases in the intensities of SNA, SSA, and TJA-1 after doxorubicin treatment (DXR+) compared with the intensities in the absence of doxorubicin treatment (DXR−) ($P < 0.05$).

Table 1. Expression Profile of Sialylated Proteins in Doxorubicin-Treated Huh7 Cells, Obtained from iTRAQ Analysis

Swiss-Prot accession number	sequence	description	gene symbol	site	115/114	115/114 count	115/114 variability [%]
Q9Y4L1	VFGSQNLTTVK	hypoxia up-regulated protein 1	*HYOU1*	N515	7.137	1	
P13674	DMSDGFISNLTIQR	prolyl 4-hydroxylase subunit alpha-1	*P4HA1*	N367	4.857	1	
P11279	SGPKNMTFDLPSDATVVLNR	lysosome-associated membrane glycoprotein 1	*LAMP1*	N562, N76	3.796	1	
O60568	SAEFFNYTVR	procollagen-lysine, 2-oxoglutarate 5-dioxygenase 3	*PLOD3*	N63	2.848	1	
O60568	EQYIHENYSR	procollagen-lysine, 2-oxoglutarate 5-dioxygenase 3	*PLOD3*	N548	2.347	1	
P11142	VEIIANDQGNR	heat shock cognate 71 kDa protein	*HSPA8*	N31	2.152	1	
P16278	NNVITLNITGK	beta-galactosidase	*GLB1*	N458, N464	1.963	1	
P11279	NMTFDLPSDATVVLNR	lysosome-associated membrane glycoprotein 1	*LAMP1*	N62, N76	1.890	1	
Q92508	ELYNGTADITLR	piezo-type mechanosensitive ion channel component 1	*PIEZO1*	N2294	1.852	1	
P11279	ENTSDPSLVIAFGR	lysosome-associated membrane glycoprotein 1	*LAMP1*	N84	1.836	2	6.0
Q86VZ4	SSDNVSVTVLR	low-density lipoprotein receptor-related protein 11	*LRP11*	N291	1.806	2	8.6
P19022	SNISILR	cadherin-2	*CDH2*	N692	1.804	1	
P13473	AASTYSIDSVSFSYNTGDNTTFPDAEDK	lysosome-associated membrane glycoprotein 2	*LAMP2*	N257	1.699	1	
Q5ZPR3	TALFPDLLAQGNASLR	CD276 antigen	*CD276*	N104	1.697	1	
P11047	TLAGENQTAFEIEELNR	laminin subunit gamma-1	*LAMC1*	N1223	1.696	1	
Q5ZPR3	QLVHSFAEGQDQGSAYANR	CD276 antigen	*CD276*	N309	1.634	1	
P13473	VQPFNVTQGK	lysosome-associated membrane glycoprotein 2	*LAMP2*	N356	1.614	2	12.5
P56199	VYVYALNQTR	integrin alpha-1	*ITGA1*	N532	1.611	1	

and fixed with methanol for 10 min at −20 °C, followed by blocking with PBS containing 1% BSA for 1 h at RT. The cells were then incubated overnight at 4 °C with the mouse antifetuin-A antibody (Santa Cruz Biotechnology) and rabbit antialbumin

dx.doi.org/10.1021/pr5004399 | J. Proteome Res. 2014, 13, 4869−4877

antibody (Rockland Immunochemicals, Gilbertsville, PA, USA). Fluorescein isothiocyanate (FITC)-conjugated SSA (J-Oil Mills, Inc., Tokyo, Japan) was incubated for 2 h at RT. Primary antibody binding was detected with Alexa-488 antimouse IgG or Alexa-546 antirabbit IgG (Invitrogen). Finally, the cells were washed three times for 2 min with PBS. Staining was evaluated using confocal microscopy.

Statistical Analysis

Statistical analyses were conducted using JMP Pro 10.0 software (SAS Institute Inc., Cary, NC, USA). Variables in lectin array analyses were expressed as the mean ± standard deviation (SD). The Wilcoxon test was used to assess any significant differences in variables. Differences were considered statistically significant at $P < 0.05$.

RESULTS

Glycan Profiling of Huh7 Cells Treated with or without DXR Using Lectin Microarray

First, we determined the DXR IC_{50} concentration in Huh7 cells treated with DXR for 48 h, using the WST assay (Nacalai Tesque, Kyoto, Japan) (data not shown). Huh7 cells were treated with the IC_{50} concentration of DXR (5 μg/mL) for 48 h, and then Cy3-labeled proteins derived from these cells were subjected to lectin microarray analysis (Figure 1). Interestingly, the intensities of three sialylated glycan-recognizing lectins (SNA, SSA, and TJA-1) among 43 lectins were significantly higher in DXR-treated cells than in untreated cells. This finding is very similar to that of our previous study, which demonstrated that hepatic CSCs (CD133 and CD13 double-positive Huh7 cells) highly expressed sialylated glycans.[16] In this previous study, we also demonstrated that SSA lectin could be used as a tool for isolating CSCs. Unexpectedly, binding to the lectins PSA and LCA was slightly decreased in DXR-treated cells. Both PSA and LCA lectins recognize α1−6 core fucosylation, which is involved in carcinogenesis. Changes in the branching formation of *N*-glycans, as judged by binding to L4-PHA lectin, were not observed in Huh7 cells treated with DXR.

Sialylated Protein Expression Profile of Huh7 Cells Treated with or without DXR

To identify target glycoproteins that show increased sialylation upon DXR treatment, iTRAQ analysis was performed. Total cell lysates from Huh7 cells treated with or without DXR were trypsinized and applied to a SSA-agarose column. Subsequently, captured sialylated glycopeptides were deglycosylated with glycopeptidase F and labeled with a specific isobaric iTRAQ reagent. A total of 191 proteins were identified with this analysis. Among these, we have listed glycoproteins that showed more than 1.6-fold expression in DXR-treated Huh7 cells as compared with that in DXR-untreated Huh7 cells (Table 1).

Western Blot Analysis of Glycoprotein Listed by iTRAQ Analysis

To further verify the changes in the glycoproteins listed in Table 1, we selected four proteins [hypoxia up-regulated protein 1 (HYOU1), prolyl 4-hydroxylase subunit alpha-1 (P4HA1), lysosomal-associated membrane glycoprotein 1 (LAMP1), and LAMP2], which are known to be abundantly glycosylated and associated with cancer, for validation using Western blotting (Figure 2). The expression levels of HYOU1 and P4HA1 showed no significant differences between Huh7 cells with or without DXR treatment. This indicates that the sialylation levels of these proteins increased with DXR treatment and total protein levels were not changed. In contrast, both LAMP1 and LAMP2 protein levels were slightly increased in DXR-treated Huh7 cells.

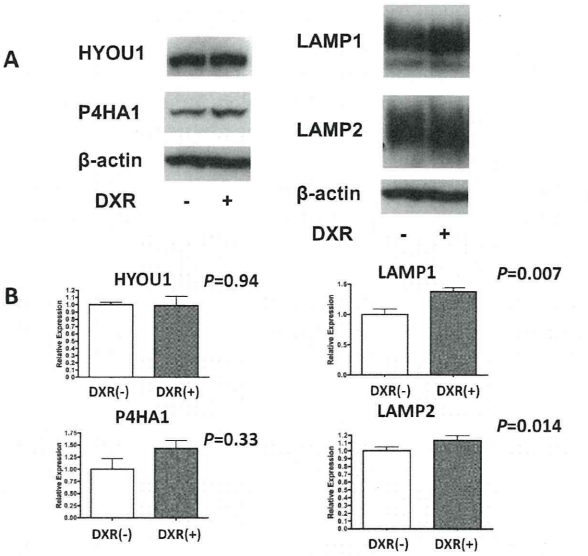

Figure 2. Western blot analyses of HYOU1, P4HA1, LAMP1, and LAMP2. (A) Twenty-five micrograms (HYOU1 and P4HA1), 10 μg (LAMP1 and β-actin), and 2.5 μg (LAMP2) of total cellular proteins were electrophoresed on 8% polyacrylamide gels, and Western blot analyses were performed. β-actin was used as the control. (B) Expression level of each protein band was determined by ImageJ64 software for three independent blots, and statistical analysis was performed by Wilcoxon test. Each result represented the mean ± SD.

Increase in Sialylation of 70 kDa Proteins in DXR-Treated Huh7 Cells

Next, we performed lectin blot analysis to determine changes in sialylation in each protein band in DXR-treated Huh7 cells. Very interestingly, dramatic increases in sialylation in approximately 70 kDa proteins were observed (Figure 3A). While other bands

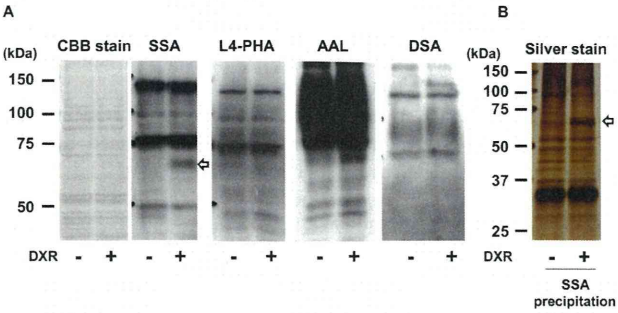

Figure 3. Lectin blot analyses and SSA precipitation of Huh7 cells treated with or without doxorubicin. (A) Lectin blot analyses using SSA, AAL, L4-PHA, and DSA. (B) Proteins were captured by SSA-agarose bead complexes, followed by 10% SDS-PAGE analysis with silver staining. The arrows indicate specifically sialylated bands. These data were results from 3−5 independent experiments.

in the SSA lectin blot were slightly increased or decreased in DXR-treated cells, the 70 kDa proteins were very prominent. Therefore, the protein levels of these 70 kDa proteins might be increased upon DXR treatment. Mechanisms that can increase sialylation in glycoproteins include increased branching, increased presence of Lewis structures, and extension of lactosamine structure repeats. L4-PHA, AAL, and DSA can recognize these glycan structures, respectively. Therefore, we examined these lectin blot analyses. The 70 kDa band was not

dx.doi.org/10.1021/pr5004399 | J. Proteome Res. 2014, 13, 4869−4877

detected in other lectin blot analyses, although a significant increase was observed in AAL lectin blot analysis (Figure 3A). The increase in the intensity of the 70 kDa band in the DXR-treated cells in the AAL blot indicates an increased presence of Lewis structures in some glycoproteins. To capture this sialylated glycoprotein at 70 kDa, SSA precipitation was performed (Figure 3B). As shown in Figure 3B, approximately 70 kDa sialylated glycoproteins were identified using SSA-agarose precipitation followed by silver staining. Next, the 70 kDa protein spot was digested with trypsin, and the extracted peptides were analyzed using LC–MS/MS. The spectra thus acquired were searched against the Swiss-Prot database with the aid of the MASCOT search engine. In this manner, we identified five proteins as candidate sialylated glycoproteins (Table 2).

Table 2. Sialylated 70 kDa Proteins Identified by LC–MS/MS

Swiss-Prot accession no.	protein	peptide matching	protein coverage (%)
P16278	beta-galactosidase	12	11.23
P02765	alpha-2-HS-glycoprotein (fetuin-A)	8	5.45
Q02413	desmoglein-1	2	0.95
Q9NPR9	protein GPR108	2	2.03
P11279	lysosome-associated membrane glycoprotein 1	1	2.64

Evaluation of the 70 kDa Sialylated Proteins in DXR-Treated Huh7 Cells by Western Blot

To evaluate the 70 kDa sialylated proteins listed in Table 1, Western blotting was performed. Because of their large hit numbers in LC–MS/MS analysis, we focused on fetuin-A and beta-galactosidase. Although the protein expression of beta-galactosidase was slightly increased in DXR-treated Huh7 cells, the protein expression of beta-galactosidase obtained by SSA precipitation was much greater in DXR-treated Huh7 cells (Figure 4A). This result indicates that the sialylation levels of beta-galactosidase increased with DXR treatment. Next, Western blot analyses of alpha-2-HS-glycoprotein (fetuin-A) were performed. Although the protein expression of fetuin-A in total cell lysate was lower in DXR-treated Huh7 cells, the protein expression of fetuin-A obtained by SSA precipitation was significantly higher in DXR-treated Huh7 cells (Figure 4B). Furthermore, the molecular weight of fetuin-A was higher in DXR-treated Huh7 cells. These results indicate that oligosaccharide structures of fetuin-A are completely different between DXR-treated and untreated Huh7 cells. Additionally, the molecular weight of fetuin-A in the conditioned medium was almost the same between DXR-treated and untreated cells, which was consistent with the sialylated fetuin-A band (70 kDa) observed in cell lysates treated with DXR (Figure 4C). We found that sialylated fetuin (70 kDa) was barely observed in untreated cell lysate and almost all of the 70 kDa fetuin was secreted into the medium in the absence of DXR treatment. In order to determine whether the changes in molecular weight of fetuin-A were due to glycosylation/sialylation, the total cell lysates of DXR-treated and untreated Huh7 cells were incubated with 200 mU/mL neuraminidase, which specifically cleaves terminal sialic acid residues. A decrease of the molecular weight of fetuin-A was observed following neuraminidase treatment, suggesting that sialylation in fetuin-A was increased upon DXR treatment (Figure 4D). Next, to determine whether the changes in fetuin-A bands were dependent on N-glycosylation, cell lysates were treated with 20 mU/mL glycopeptidase F, which removes most complex type N-linked carbohydrates from glycoproteins. As expected, the fetuin-A band was decreased following this treatment (Figure 4D).

Localization of Fetuin-A in Huh7 Cells Treated with DXR

To examine the localization of fetuin-A in DXR-treated Huh7 cells, an immunofluorescence study was performed. Cells were stained with antifetuin-A antibody (Figure 5A,B), and anti-albumin antibody, which served as a nonglycosylated secretory protein control (Figure 5A) and SSA (Figure 5B). Although the expression of fetuin-A was lower in DXR-treated Huh7 cells than in untreated cells, colocalization of fetuin-A and albumin were observed in DXR-treated and untreated cells. In contrast, the localization of SSA changed dramatically in DXR-treated cells (Figure 5B). The localization of these signals was altered in DXR-treated cells from a perinuclear pattern to a scatter pattern in the cytoplasm. SSA and fetuin-A were not colocalized in DXR-untreated cells, but a few DXR-treated cells showed colocalization of SSA and fetuin-A (Figure 5B).

■ DISCUSSION

In the present study, to identify target glycoproteins for SSA lectin, we first used iTRAQ systems with SSA-agarose capture. However, the amounts of cellular proteins that could be isolated using CD133 antibody and SSA lectin were too small for proteomic analyses. Therefore, we used the anticancer drug DXR. Theoretically, treatment with DXR at its IC_{50} can concentrate CSCs. Lectin array analyses showed increased binding to SSA, SNA, and TJA-1 in DXR-treated Huh7 cells. Similar results were obtained in CD133 and CD13 double-positive CSCs derived from Huh7 cells.[16] These findings suggest that Huh7 cells treated with DXR display similar characteristics to CSCs. SSA, SNA, and TJA-1 recognize terminal α2, 6-sialic acid residues. We speculate that this increased sialylation in DXR-treated Huh7 cells might have potential benefits for the survival of anticancer drug-treated cells. To identify those glycoproteins that are targets for sialylation, iTRAQ analysis was performed. Of the 19 candidate glycoproteins we identified, concentration of HYOU1 was much greater than those of the other glycoproteins. HYOU1 plays an important role in hypoxia/ischemia and angiogenesis. HYOU1 is overexpressed in invasive breast cancer, and its overexpression appears to be associated with poor prognosis.[35] A high score in iTRAQ analyses using SSA agarose capture may indicate one of two possibilities: an increase in the glycoprotein level itself or an increase in sialic acid levels in a specific glycoprotein. Protein levels remain unchanged in the case of HYOU1 (Figure 2). Although we would have liked to perform immunoprecipitation followed by SSA lectin blotting, the antibody for immunoprecipitation was not available. We predict that sialic acid increases in HYOU1 in DXR-treated Huh7 cells. The next high score in iTRAQ analysis was that of P4HA1. P4HA1 plays a central role in collagen synthesis. P4HA1 has also been shown to be expressed in hepatocellular carcinoma tissue. In contrast, the protein expression levels of LAMP1 and LAMP2 were increased with DXR treatment. LAMP1 and LAMP2 are localized primarily in the periphery of lysosomes and are recognized as major constituents of the lysosomal membrane.[36] It is well-known that these molecules are among the most heavily glycosylated cellular proteins, with approximately 50% of their mass being carbohydrates. Therefore, these proteins could be captured by an SSA-agarose column and detected using iTRAQ analysis. Since these 4 glycoproteins are associated with cancer progression as well as metastasis, increases in sialic acid content

dx.doi.org/10.1021/pr5004399 | J. Proteome Res. 2014, 13, 4869–4877

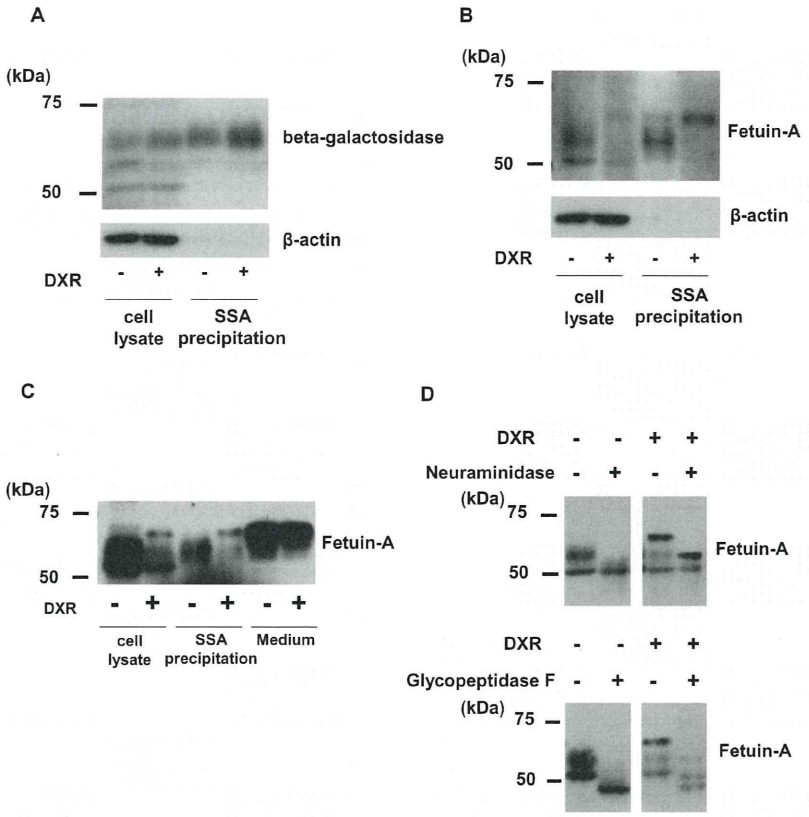

Figure 4. Evaluation of 70 kDa sialylated proteins in Huh7 cells treated with doxorubicin with Western blotting. (A) Ten micrograms of cell lysate and total cellular proteins obtained from lectin precipitation (50 μg) were electrophoresed on 8% acrylamide gels, and Western blot analyses of beta-galactosidase were performed. (B) Western blotting analysis of fetuin-A was performed. (C) Western blotting analysis of fetuin-A from Huh7 cell lysates (30 μg) and conditioned media (1 μL) in the presence or absence of DXR treatment. (D) Cell lysates were treated with neuraminidase or glycopeptidase F at 37 °C overnight. The lysates were then subjected to 8% SDS-PAGE analysis. These data were results from 3 independent experiments.

in these proteins can change biological characteristics, including cancer stemness.

Next, we conducted an SSA lectin blot analysis to determine total/partial increases in sialic acid content in DXR-treated Huh7 cells. Surprisingly, proteins approximately 70 kDa in mass were specifically sialylated. From LC–MS/MS analyses, we identified five proteins that were not identified by iTRAQ analysis, with the exception of LAMP1. Fetuin-A (predicted molecular weight: 38 kDa), GPR108 (predicted molecular weight: 60 kDa), LAMP1 (predicted molecular weight: 45 kDa), and LAMP2 (predicted molecular weight: 45 kDa) are abundantly glycosylated. In our study, 70 kDa fetuin-A was heavily sialylated. Therefore, the band sizes of fetuin-A, GPR108, LAMP1, and LAMP2 were heavier than the predicted molecular weights. In addition, the predicted size of beta-galactosidase is about 116 kDa, but the alternatively spliced variant of beta-galactosidase was reported to be about 67 kDa.[37] Desmoglein-1 (predicted molecular weight: 112 kDa) would be cleaved by DXR-activated proteases. The reason why these proteins were not identified by iTRAQ is likely due to the analysis method of iTRAQ. Because proteins are cleaved into peptides in iTRAQ analysis, the steric structures of each protein is not reflected in iTRAQ analysis. In contrast, the steric structures of each protein and the site of *N*-glycan attachment are necessary in SSA precipitation analysis. These differences between iTRAQ and SSA precipitation are likely the reason for the different results seen in our study.

In LC–MS/MS analysis, we focused on beta-galactosidase and fetuin-A because of their predominantly large hit numbers. Beta-galactosidase (lysosomal hydrolase) cleaves the terminal beta-galactose from glycoconjugates. It is reported that anticancer drug treatment induces a senescence-like phenotype, and senescent cells are characterized by the appearance of senescence-associated beta-galactosidase.[38] Therefore, increases in sialic acid in beta-galactosidase in DXR-treated Huh7 cells are very interesting. Another glycoprotein, identified as a 70 kDa sialylated glycoprotein, was fetuin-A. Fetuin-A is well-known as a heavily sialylated glycoprotein with both N-linked and O-linked carbohydrate side chains.[39,40] Although various previous reports have discussed the biological functions of fetuin-A,[41,42] no studies have demonstrated differences in fetuin-A functions due to glycosylation differences. Asialofetuin-A is well-known to bind easily to galectin-3, while sialylated fetuin (sialofetuin) is reported to have no binding ability to galectin-3.[43,44] These biological differences would contribute to the functional diversity of variously glycosylated fetuin-A.

Neuraminidase treatment decreases the molecular weight of fetuin-A in DXR-treated Huh7 cells, and the lowered molecular weight was consistent with that of fetuin-A in DXR-untreated Huh7 cells, suggesting that fetuin-A was heavily sialylated in DXR-treated Huh7 cells. The question arises as to why this sialylated fetuin-A was not secreted into the conditioned medium. Therefore, we performed immunocytochemical analysis using confocal microscopy. Most of the fetuin-A was colocalized with albumin in DXR-treated cells compared to untreated cells, indicating that the secreted proteins were in the same endosome as during DXR treatment. A previous study

dx.doi.org/10.1021/pr5004399 | J. Proteome Res. 2014, 13, 4869–4877

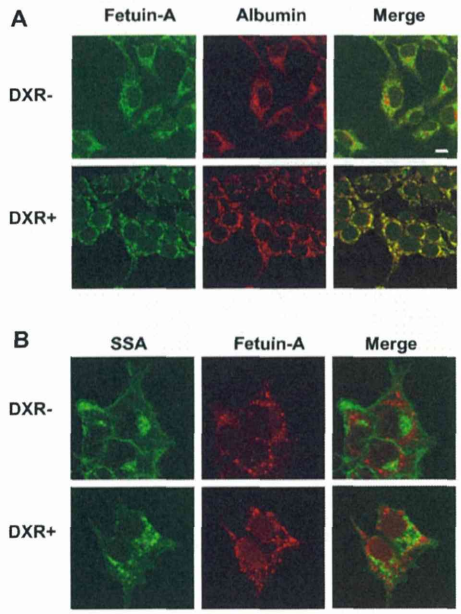

Figure 5. Localization of fetuin-A in Huh7 cells treated with doxorubicin. Immunocytochemical analyses were performed in Huh7 cells treated with or without DXR. After fixation of the cells, staining signals were visualized by laser scanning confocal microscopy. (A) Fetuin-A was visualized by Alexa-488-labeled immunostaining (green), albumin was visualized by Alexa-546-labeled immunostaining (red). (B) SSA was visualized by FITC labeling (green), and fetuin-A was visualized by Alexa-546-labeled immunostaining (red). The magnification is ×120. The bar indicates 10 μm. These data were results from 3 independent experiments.

showed that DXR induced apoptosis at a high dose (IC_{90}) but induced autophagy at a low dose (IC_{50}).[45] However, fetuin-A was not located in either the lysosome or the autophagosome (data not shown). Next we examined immunostaining of SSA to detect sialylated proteins. Surprisingly, SSA staining was dramatically changed, and a few cells showed colocalization of fetuin-A and SSA in DXR-treated cells. These results indicate that a small amount of sialylated fetuin-A remained inside the cell in DXR-treated cells. In general, fetuin-A is known as a highly sialylated serum protein.[46] Most sialylated fetuin-A might be promptly secreted to the conditioned medium (Figure 4C). In contrast, a small amount of sialylated fetuin-A remained inside the cell in DXR-treated cells. Further studies should be performed using sialyltransferase knockout or knockdown cells to evaluate the relationship between sialylation and the localization of glycoproteins, especially that of fetuin-A in anticancer drug treated cells. Since sialylation is a glycomarker for stem cells,[16,47] changes in the localization of sialylated proteins in CSCs might be involved in stem cell biology.

■ ASSOCIATED CONTENT

Supporting Information

Proliferation of CD133 positive Huh7 cells (SSA positive (+) or negative (−)) under 5-FU treatment. Raw data of MS/MS analysis. List of the glycoproteins identified in iTRAQ analysis. This material is available free of charge via the Internet at http://pubs.acs.org.

■ AUTHOR INFORMATION

Corresponding Author

*(E.M.) Tel/Fax: +81-6-6879-2590. E-mail: emiyoshi@sahs.med.osaka-u.ac.jp.

Notes

The authors declare no competing financial interest.

■ ACKNOWLEDGMENTS

This study was supported by a Grant-in-Aid for Scientific Research (A), No. 21249038, from the Japan Society for the Promotion of Science, and partially supported as a research program of the Project for Development of Innovative Research on Cancer Therapeutics (P-Direct), Ministry of Education, Culture, Sports, Science and Technology of Japan.

■ ABBREVIATIONS

CSCs, cancer stem cells; DXR, doxorubicin; SSA, *Sambucus sieboldiana* agglutinin; SNA, *Sambucus nigra* lectin; TJA-1, *Tricosanthes japonica* agglutinin-1; PSA, *Pisum sativum* agglutinin; LCA, *Lens culinaris* agglutinin; WGA, Wheat germ agglutinin; L4-PHA, *Leukoagglutinating phytohemagglutinin*; AAL, *Aleuria aurantia* lectin; DSA, *Datura stramonium agglutinin*; iTRAQ, isobaric tags for relative and absolute quantitation; HYOU1, hypoxia up-regulated protein 1; P4HA1, prolyl 4-hydroxylase subunit alpha-1; LAMP1, lysosomal-associated membrane glycoprotein 1

■ REFERENCES

(1) Reya, T.; Morrison, S. J.; Clarke, M. F.; Weissman, I. L. Stem cells, cancer, and cancer stem cells. *Nature* **2001**, *414* (6859), 105–11.
(2) Ailles, L. E.; Weissman, I. L. Cancer stem cells in solid tumors. *Curr. Opin. Biotechnol.* **2007**, *18* (5), 460–6.
(3) Mertins, S. D. Cancer stem cells: a systems biology view of their role in prognosis and therapy. *Anticancer Drugs* **2014**, *25* (4), 353–67.
(4) Dean, M.; Fojo, T.; Bates, S. Tumour stem cells and drug resistance. *Nat. Rev. Cancer* **2005**, *5* (4), 275–84.
(5) Bao, S.; Wu, Q.; McLendon, R. E.; Hao, Y.; Shi, Q.; Hjelmeland, A. B.; Dewhirst, M. W.; Bigner, D. D.; Rich, J. N. Glioma stem cells promote radioresistance by preferential activation of the DNA damage response. *Nature* **2006**, *444* (7120), 756–60.
(6) Malik, B.; Nie, D. Cancer stem cells and resistance to chemo and radio therapy. *Front. Biosci., Elite Ed.* **2012**, *4*, 2142–9.
(7) Baumann, M.; Krause, M.; Thames, H.; Trott, K.; Zips, D. Cancer stem cells and radiotherapy. *Int. J. Radiat. Biol.* **2009**, *85* (5), 391–402.
(8) Haraguchi, N.; Ishii, H.; Mimori, K.; Tanaka, F.; Ohkuma, M.; Kim, H. M.; Akita, H.; Takiuchi, D.; Hatano, H.; Nagano, H.; Barnard, G. F.; Doki, Y.; Mori, M. CD13 is a therapeutic target in human liver cancer stem cells. *J. Clin. Invest.* **2010**, *120* (9), 3326–39.
(9) Zhu, Z.; Hao, X.; Yan, M.; Yao, M.; Ge, C.; Gu, J.; Li, J. Cancer stem/progenitor cells are highly enriched in CD133+CD44+ population in hepatocellular carcinoma. *Int. J. Cancer* **2010**, *126* (9), 2067–78.
(10) Yang, Z. F.; Ho, D. W.; Ng, M. N.; Lau, C. K.; Yu, W. C.; Ngai, P.; Chu, P. W.; Lam, C. T.; Poon, R. T.; Fan, S. T. Significance of CD90+ cancer stem cells in human liver cancer. *Cancer Cell* **2008**, *13* (2), 153–66.
(11) Al-Hajj, M.; Wicha, M. S.; Benito-Hernandez, A.; Morrison, S. J.; Clarke, M. F. Prospective identification of tumorigenic breast cancer cells. *Proc. Natl. Acad. Sci. U.S.A.* **2003**, *100* (7), 3983–8.
(12) Kojima, K.; Musch, M. W.; Ren, H.; Boone, D. L.; Hendrickson, B. A.; Ma, A.; Chang, E. B. Enteric flora and lymphocyte-derived cytokines determine expression of heat shock proteins in mouse colonic epithelial cells. *Gastroenterology* **2003**, *124* (5), 1395–407.
(13) Ding, W.; Mouzaki, M.; You, H.; Laird, J. C.; Mato, J.; Lu, S. C.; Rountree, C. B. CD133+ liver cancer stem cells from methionine adenosyl transferase 1A-deficient mice demonstrate resistance to transforming growth factor (TGF)-beta-induced apoptosis. *Hepatology* **2009**, *49* (4), 1277–86.
(14) Fuster, M. M.; Esko, J. D. The sweet and sour of cancer: glycans as novel therapeutic targets. *Nat. Rev. Cancer* **2005**, *5* (7), 526–42.

(15) Haltiwanger, R. S.; Lowe, J. B. Role of glycosylation in development. *Annu. Rev. Biochem.* **2004**, *73*, 491–537.
(16) Moriwaki, K.; Okudo, K.; Haraguchi, N.; Takeishi, S.; Sawaki, H.; Narimatsu, H.; Tanemura, M.; Ishii, H.; Mori, M.; Miyoshi, E. Combination use of anti-CD133 antibody and SSA lectin can effectively enrich cells with high tumorigenicity. *Cancer Sci.* **2011**, *102* (6), 1164–70.
(17) Varki, A. Sialic acids in human health and disease. *Trends Mol. Med.* **2008**, *14* (8), 351–60.
(18) Yogeeswaran, G.; Salk, P. L. Metastatic potential is positively correlated with cell surface sialylation of cultured murine tumor cell lines. *Science* **1981**, *212* (4502), 1514–6.
(19) Fogel, M.; Altevogt, P.; Schirrmacher, V. Metastatic potential severely altered by changes in tumor cell adhesiveness and cell-surface sialylation. *J. Exp. Med.* **1983**, *157* (1), 371–6.
(20) Passaniti, A.; Hart, G. W. Cell surface sialylation and tumor metastasis. Metastatic potential of B16 melanoma variants correlates with their relative numbers of specific penultimate oligosaccharide structures. *J. Biol. Chem.* **1988**, *263* (16), 7591–603.
(21) Cui, H.; Lin, Y.; Yue, L.; Zhao, X.; Liu, J. Differential expression of the alpha2,3-sialic acid residues in breast cancer is associated with metastatic potential. *Oncol. Rep.* **2011**, *25* (5), 1365–71.
(22) Babal, P.; Janega, P.; Cerna, A.; Kholova, I.; Brabencova, E. Neoplastic transformation of the thyroid gland is accompanied by changes in cellular sialylation. *Acta Histochem.* **2006**, *108* (2), 133–40.
(23) Sethi, M. K.; Thaysen-Andersen, M.; Smith, J. T.; Baker, M. S.; Packer, N. H.; Hancock, W. S.; Fanayan, S. Comparative N-glycan profiling of colorectal cancer cell lines reveals unique bisecting GlcNAc and alpha-2,3-linked sialic acid determinants are associated with membrane proteins of the more metastatic/aggressive cell lines. *J. Proteome Res.* **2014**, *13* (1), 277–88.
(24) Lanctot, P. M.; Gage, F. H.; Varki, A. P. The glycans of stem cells. *Curr. Opin. Chem. Biol.* **2007**, *11* (4), 373–80.
(25) Taniguchi, N.; Ekuni, A.; Ko, J. H.; Miyoshi, E.; Ikeda, Y.; Ihara, Y.; Nishikawa, A.; Honke, K.; Takahashi, M. A glycomic approach to the identification and characterization of glycoprotein function in cells transfected with glycosyltransferase genes. *Proteomics* **2001**, *1* (2), 239–47.
(26) Hermann, P. C.; Huber, S. L.; Herrler, T.; Aicher, A.; Ellwart, J. W.; Guba, M.; Bruns, C. J.; Heeschen, C. Distinct populations of cancer stem cells determine tumor growth and metastatic activity in human pancreatic cancer. *Cell Stem Cell* **2007**, *1* (3), 313–23.
(27) Ross, P. L.; Huang, Y. N.; Marchese, J. N.; Williamson, B.; Parker, K.; Hattan, S.; Khainovski, N.; Pillai, S.; Dey, S.; Daniels, S.; Purkayastha, S.; Juhasz, P.; Martin, S.; Bartlet-Jones, M.; He, F.; Jacobson, A.; Pappin, D. J. Multiplexed protein quantitation in Saccharomyces cerevisiae using amine-reactive isobaric tagging reagents. *Mol. Cell Proteomics* **2004**, *3* (12), 1154–69.
(28) Zieske, L. R. A perspective on the use of iTRAQ reagent technology for protein complex and profiling studies. *J. Exp. Bot* **2006**, *57* (7), 1501–8.
(29) Kuno, A.; Uchiyama, N.; Koseki-Kuno, S.; Ebe, Y.; Takashima, S.; Yamada, M.; Hirabayashi, J. Evanescent-field fluorescence-assisted lectin microarray: a new strategy for glycan profiling. *Nat. Methods* **2005**, *2* (11), 851–6.
(30) Serada, S.; Fujimoto, M.; Ogata, A.; Terabe, F.; Hirano, T.; Iijima, H.; Shinzaki, S.; Nishikawa, T.; Ohkawara, T.; Iwahori, K.; Ohguro, N.; Kishimoto, T.; Naka, T. iTRAQ-based proteomic identification of leucine-rich alpha-2 glycoprotein as a novel inflammatory biomarker in autoimmune diseases. *Ann. Rheum. Dis.* **2010**, *69* (4), 770–4.
(31) Serada, S.; Fujimoto, M.; Takahashi, T.; He, P.; Hayashi, A.; Tanaka, T.; Hagihara, K.; Yamadori, T.; Mochizuki, M.; Norioka, N.; Norioka, S.; Kawase, I.; Naka, T. Proteomic analysis of autoantigens associated with systemic lupus erythematosus: Anti-aldolase A antibody as a potential marker of lupus nephritis. *Proteomics Clin. Appl.* **2007**, *1* (2), 185–91.
(32) He, P.; Naka, T.; Serada, S.; Fujimoto, M.; Tanaka, T.; Hashimoto, S.; Shima, Y.; Yamadori, T.; Suzuki, H.; Hirashima, T.; Matsui, K.; Shiono, H.; Okumura, M.; Nishida, T.; Tachibana, I.; Norioka, N.; Norioka, S.; Kawase, I. Proteomics-based identification of alpha-enolase as a tumor antigen in non-small lung cancer. *Cancer Sci.* **2007**, *98* (8), 1234–40.
(33) Shevchenko, A.; Wilm, M.; Vorm, O.; Mann, M. Mass spectrometric sequencing of proteins silver-stained polyacrylamide gels. *Anal. Chem.* **1996**, *68* (5), 850–8.
(34) Kuwamoto, K.; Takeda, Y.; Shirai, A.; Nakagawa, T.; Takeishi, S.; Ihara, S.; Miyamoto, Y.; Shinzaki, S.; Ko, J. H.; Miyoshi, E. Identification of various types of alpha2-HS glycoprotein in sera of patients with pancreatic cancer: Possible implication in resistance to protease treatment. *Mol. Med. Rep* **2010**, *3* (4), 651–6.
(35) Stojadinovic, A.; Hooke, J. A.; Shriver, C. D.; Nissan, A.; Kovatich, A. J.; Kao, T. C.; Ponniah, S.; Peoples, G. E.; Moroni, M. HYOU1/Orp150 expression in breast cancer. *Med. Sci. Monit* **2007**, *13* (11), BR231–239.
(36) Fukuda, M.; Viitala, J.; Matteson, J.; Carlsson, S. R. Cloning of cDNAs encoding human lysosomal membrane glycoproteins, h-lamp-1 and h-lamp-2. Comparison of their deduced amino acid sequences. *J. Biol. Chem.* **1988**, *263* (35), 18920–8.
(37) Privitera, S.; Prody, C. A.; Callahan, J. W.; Hinek, A. The 67-kDa enzymatically inactive alternatively spliced variant of beta-galactosidase is identical to the elastin/laminin-binding protein. *J. Biol. Chem.* **1998**, *273* (11), 6319–26.
(38) Eom, Y. W.; Kim, M. A.; Park, S. S.; Goo, M. J.; Kwon, H. J.; Sohn, S.; Kim, W. H.; Yoon, G.; Choi, K. S. Two distinct modes of cell death induced by doxorubicin: apoptosis and cell death through mitotic catastrophe accompanied by senescence-like phenotype. *Oncogene* **2005**, *24* (30), 4765–77.
(39) Hayase, T.; Rice, K. G.; Dziegielewska, K. M.; Kuhlenschmidt, M.; Reilly, T.; Lee, Y. C. Comparison of N-glycosides of fetuins from different species and human alpha 2-HS-glycoprotein. *Biochemistry* **1992**, *31* (20), 4915–21.
(40) Edge, A. S.; Spiro, R. G. Presence of an O-glycosidically linked hexasaccharide in fetuin. *J. Biol. Chem.* **1987**, *262* (33), 16135–41.
(41) Stefan, N.; Haring, H. U. The role of hepatokines in metabolism. *Nat. Rev. Endocrinol.* **2013**, *9* (3), 144–52.
(42) Wang, H.; Sama, A. E. Anti-inflammatory role of fetuin-A in injury and infection. *Curr. Mol. Med.* **2012**, *12* (5), 625–33.
(43) Inohara, H.; Raz, A. Identification of human melanoma cellular and secreted ligands for galectin-3. *Biochem. Biophys. Res. Commun.* **1994**, *201* (3), 1366–75.
(44) von Mach, T.; Carlsson, M. C.; Straube, T.; Nilsson, U.; Leffler, H.; Jacob, R. Ligand binding and complex formation of galectin-3 is modulated by pH variations. *Biochem. J.* **2014**, *457* (1), 107–15.
(45) Akar, U.; Chaves-Reyez, A.; Barria, M.; Tari, A.; Sanguino, A.; Kondo, Y.; Kondo, S.; Arun, B.; Lopez-Berestein, G.; Ozpolat, B. Silencing of Bcl-2 expression by small interfering RNA induces autophagic cell death in MCF-7 breast cancer cells. *Autophagy* **2008**, *4* (5), 669–79.
(46) Ohnishi, T.; Nakamura, O.; Ozawa, M.; Arakaki, N.; Muramatsu, T.; Daikuhara, Y. Molecular cloning and sequence analysis of cDNA for a 59 kD bone sialoprotein of the rat: demonstration that it is a counterpart of human alpha 2-HS glycoprotein and bovine fetuin. *J. Bone Miner. Res.* **1993**, *8* (3), 367–77.
(47) Martin, M. J.; Muotri, A.; Gage, F.; Varki, A. Human embryonic stem cells express an immunogenic nonhuman sialic acid. *Nat. Med.* **2005**, *11* (2), 228–32.

Annexin A4 induces platinum resistance in a chloride-and calcium-dependent manner

Akiko Morimoto[1,2], Satoshi Serada[2], Takayuki Enomoto[3], Ayako Kim[2], Shinya Matsuzaki[1] ,Tsuyoshi Takahashi[2,4] ,Yutaka Ueda[1], Kiyoshi Yoshino[1], Masami Fujita[1], Minoru Fujimoto[2], Tadashi Kimura[1] and Tetsuji Naka[2]

[1] Department of Obstetrics and Gynecology, Osaka University Graduate School of Medicine, Japan

[2] Laboratory for Immune Signals, National Institute of Biomedical Innovation, Japan

[3] Department of Obstetrics and Gynecology, Niigata University Medical School, Japan

[4] Department of Surgery, Osaka University Graduate School of Medicine, Japan

Correspondence to: *Tetsuji Naka* , ***email***: *tnaka@nibio.go.jp*

Keywords: Annexin A4; platinum resistance; annexin repeat; chloride ion

Received: *April 04, 2014* ***Accepted***: *August 03, 2014* ***Published***: *August 04, 2014*

This is an open-access article distributed under the terms of the Creative Commons Attribution License, which permits unrestricted use, distribution, and reproduction in any medium, provided the original author and source are credited.

ABSTRACT

Platinum resistance has long been a major issue in the treatment of various cancers. We previously reported that enhanced annexin A4 (ANXA4) expression, a Ca^{2+}-regulated phospholipid-binding protein, induces chemoresistance to platinum-based drugs. In this study, we investigated the role of annexin repeats, a conserved structure of all the annexin family, responsible for platinum-resistance as well as the effect of knockdown of ANXA4. ANXA4 knockdown increased sensitivity to platinum-based drugs both *in vitro* and *in vivo*. To identify the domain responsible for chemoresistance, ANXA4 deletion mutants were constructed by deleting annexin repeats one by one from the C terminus. Platinum resistance was induced both *in vitro* and *in vivo* in cells expressing either full-length ANXA4 or the deletion mutants, containing at least one intact annexin repeat. However, cells expressing the mutant without any calcium-binding sites in the annexin repeated sequence, which is essential for ANXA4 translocation from the cytosol to plasma membrane, failed to acquire platinum resistance. After cisplatin treatment, the intracellular chloride ion concentration, whose channel is partly regulated by ANXA4, significantly increased in the platinum-resistant cells. These findings indicate that the calcium-binding site in the annexin repeat induces chemoresistance to the platinum-based drug by elevating the intracellular chloride concentration.

INTRODUCTION

Since cisplatin was first introduced as an anticancer drug in the 1970s [1], various platinum-based drugs have been developed and widely used not only against gynecological but also against other cancers, including lung, colorectal, testicular, prostate and bladder cancer [2-6]. Although these platinum-based drugs have significantly contributed to improve survival rates, chemoresistance to these drugs has become a major problem in recent years [7-9]. It has now been elucidated that the mechanism of platinum resistance is mediated by reduced platinum accumulation, increased platinum detoxification, increased repair of platinum–DNA adducts and inhibited apoptosis [10-12]. Several proteins have been reported to be candidate factors such as copper transporters: CTR1[13], ATP7A and ATP7B[14-17]; multidrug resistance protein 2 (MRP2) [18-20]; glutathione S-transferase enzyme π (GSTπ) [21]; excision cross-complementing gene 1 (ERCC1) [22]; receptor-interacting protein 1 (RIP1) [23]; microRNAs [24-26]; and p53 [27]. In contrast, there are still several proteins related to platinum resistance without a full understanding of how these proteins help cells to confer platinum-based drugs.

We recently reported that annexin A4 (ANXA4) is overexpressed in ovarian clear cell carcinoma and

induces chemoresistance to platinum-based drugs [28]. Annexins are calcium-regulated and negatively charged phospholipid membrane-binding proteins. The basic structure of annexins consists of 2 major domains: a conserved structural element called an annexin repeat, a segment of 70 amino acid residues at the C terminus, and the N-terminal region unique for a given member of the family and determining individual annexin properties *in vivo*. The annexin repeat possesses the calcium and membrane binding sites and is responsible for mediating the canonical membrane binding properties [29]. These domains in ANXA4 are surrounded by relatively short amino and carboxy termini that do not have any known function [30]. ANXA4 is involved in membrane permeability, exocytosis and regulation of chloride channels in a calcium-dependent manner [29, 31-33]. ANXA4 is almost exclusively expressed in epithelial cells [34]. With regard to cancer, ANXA4 overexpression has been reported in various tumours, such as lung, gastric, colorectal, renal, pancreatic, ovarian and prostate cancer [28, 35-39] and is associated with tumour invasiveness, metastasis and chemoresistance [37, 40]. Moreover, ANXA4 has been shown to be associated with resistance to platinum-based drugs [28, 41-43].

ANXA4-induced platinum resistance appears to be mediated in part by the increased extracellular efflux of platinum mediated by the copper transporter ATP7A[28, 44]. Another mechanism of ANXA4-induced chemoresistance is the modulation of NF-κB transcriptional activity [45]. ANXA4 suppresses NF-κB transcriptional activity through interaction with the p50 subunit in a calcium-dependent manner; ANXA4 causes resistance to apoptosis induction by etoposide.

While ANXA4 prominently associated with chemoresistance, the functional domain of ANXA4 remains unclear. Therefore, to clarify the functional domain of ANXA4 is required to understand detailed mechanisms of the chemoresistance induced by ANXA4 and also overcome chemoresistance. In this study, focusing on platinum resistance, we aimed to identify the ANXA4 domain relevant to chemoresistance with regard to its structure as well as to test whether knockdown of ANXA4 expression could improve platinum resistance. Our data showed that the annexin repeat plays an important role in platinum resistance induced by ANXA4, which occurs in a calcium-dependent manner.

RESULTS

Establishment of ANXA4 knockdown RMG-I cells

To create cell lines with a stable ANXA4 knockdown, we analysed ANXA4 expression in ovarian cancer cells using western blotting. ANXA4 expression was strong in clear cell carcinoma cell lines (OVTOKO, OVISE and RMG-I) compared with serous adenocarcinoma cell lines (A2780, OVCAR3 and OVSAHO) and a mucinous adenocarcinoma cell line (MCAS; Fig. 1A). To see whether blocking ANXA4 expression was a valid chemosensitising strategy for ovarian clear cell carcinoma treatment, ANXA4 was stably suppressed using an ANXA4 shRNA plasmid. We established RMG-I-Y4 and R5 cell clones as well as RMG-I NC7 cell clones transfected with the empty vector as a control. Compared with RMG-I NC7 and untransfected control parent RMG-I cells, ANXA4 expression was markedly down-regulated at the protein level in RMG-I-Y4 and RMG-I-R5 cells (Fig. 1B). In the absence of any drug treatment, the growth rate among the 4 cell lines was similar *in vitro* (data not shown).

Knockdown of ANXA4 expression enhances sensitivity to cisplatin and carboplatin

The sensitivity to cisplatin and carboplatin was assessed in the 3 RMG-I clones NC7, R5 and Y4. Compared with the IC_{50} for cisplatin in NC7 cells, IC_{50} was significantly decreased in Y4 cells and R5 cells ($p < 0.01$; Fig. 1C, left panel). Similarly, IC_{50} for carboplatin significantly decreased in Y4 cells and R5 cells compared with NC7 cells ($p < 0.01$; Fig. 1C, right panel). IC_{50} for cisplatin and carboplatin decreased approximately 2-fold because of the knockdown of ANXA4 expression.

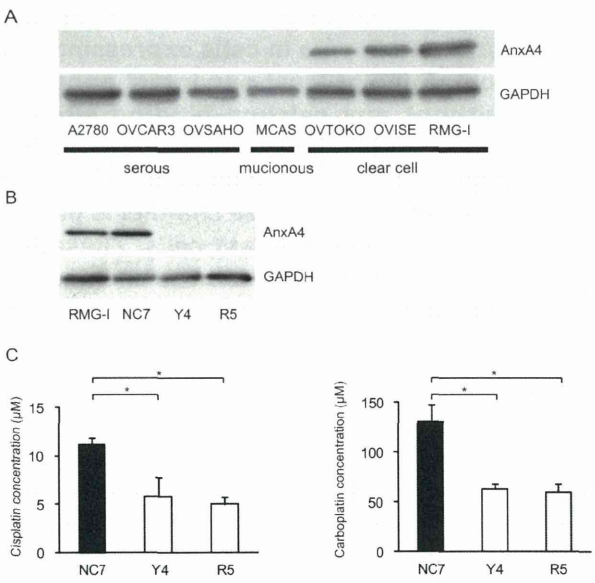

Fig.1: Knockdown of ANXA4 expression attenuates platinum resistance. (A) ANXA4 expression in indicated ovarian cancer cell lines and (B) established ANXA4 knockdown RMG-I cells (R5 and Y4) was confirmed using Western blotting. (C) IC_{50} for both cisplatin and carboplatin was significantly reduced in R5 and Y4 cells compared with NC7 cells. Data are presented as mean ± SD (*$p < 0.01$).

Suppression of ANXA4 expression improves platinum sensitivity *in vivo*

To determine whether ANXA4 knockdown in clear cell carcinoma cells improved platinum sensitivity *in vivo*, NC7 and Y4 cells were subcutaneously injected in ICR *nu/nu* mice. One week after inoculation with the tumour cells, the mice were randomised into 2 groups and received cisplatin or PBS *i.p.* twice a week for 4 weeks. The tumour growth rate in the absence of drugs was similar for both cell lines (Figs. 2A and 2B). Cisplatin treatment had very little effect on NC7 cells (Fig. 2A), but tumour volume markedly decreased in Y4 cells (Fig. 2B). Cisplatin treatment significantly decreased tumour growth in Y4 cells (87.4 ± 1.8%) compared with NC7 cells (-1.1 ± 18.0%; $p < 0.01$; Fig. 2C). These results showed that ANXA4 knockdown in the RMG-I cell line significantly attenuated resistance to cisplatin *in vivo*.

The annexin repeat domain is required for the platinum drug resistance

To identify a possible resistance-related domain within the annexin repeated sequence of ANXA4, we constructed 3 deletion mutants by deleting the annexin repeats one by one from the C-terminal region. Figure 3A shows the structure of each deletion mutant. Full-length ANXA4, 3 ANXA4 deletion mutants or the empty vector were transfected into NUGC3 cells, whose endogenous ANXA4 expression is relatively low (Supplementary Fig. S1). Therefore, we established cell lines stably overexpressing full-length ANXA4 (FL-22), each ANXA4 deletion mutant (R3-6, R2-13 or R1-12) or the empty vector (NC-14). Expression of each ANXA4 deletion mutant was confirmed using Western blotting (Fig. 3B).

Subsequently, the sensitivity to the platinum-based drugs cisplatin and carboplatin was assessed. Cells transfected with full-length ANXA4 and the 3 deletion ANXA4 mutants were significantly more resistant to both cisplatin and carboplatin compared with control cells, approximately with a 1.7- to 2.2-fold increase in IC_{50} for cisplatin ($p < 0.01$) and a 1.4- to 1.7-fold increase in IC_{50} for carboplatin ($p < 0.05$; Fig. 3C).

To test whether these deletion mutants induce platinum resistance through regulating cellular drug concentration as previously reported [28], we quantitated the intracellular platinum content of each deletion mutant-transfected cell clone after cisplatin treatment, which is one of the most representative platinum drugs. Platinum accumulation was significantly reduced in cells overexpressing either full-length ANXA4 or any of the 3

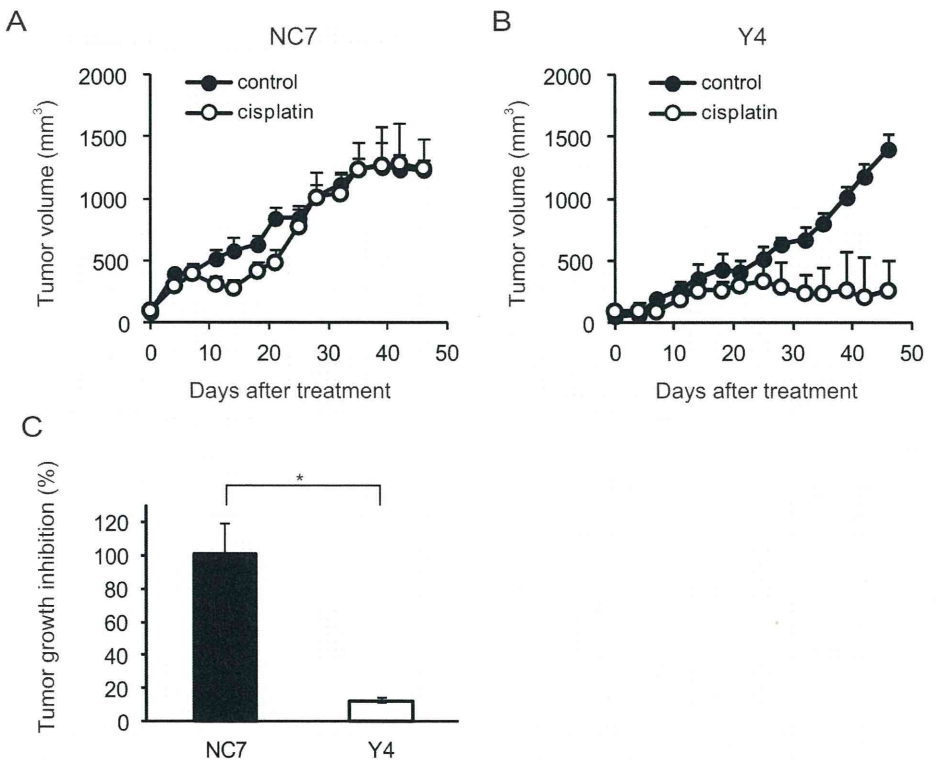

Fig.2: ANXA4 knockdown cells show enhanced sensitivity to cisplatin *in vivo*. Female ICR *nu/nu* mice were subcutaneously inoculated with RMG-I NC7 or Y4 cells and given PBS (control group: *filled circles*) or cisplatin i.p. (3 mg/kg; treatment group: *open circles*) twice weekly for 4 weeks (n = 6 per group). Growth curves of NC7 tumours (A) and Y4 tumours (B). The mean volume (points) ± SE (bars) is shown. (C) Comparison of the cisplatin-induced growth inhibition of tumours 46 days after treatment among NC7 and Y4 tumours. The average (columns) ± SE (bars) are shown (*$p < 0.01$).

deletion mutants compared with NC-14 cells regardless of the incubation time after cisplatin exposure (Fig. 3D). These results suggested that the decreased intracellular platinum contents were associated with platinum resistance of the cells transfected with ANXA4 full length and each deletion mutant.

The calcium-binding site of the annexin repeat is responsible for platinum resistance

As specified above, platinum resistance was enhanced in cells overexpressing ANXA4 deletion mutants, which contained at least 1 intact annexin repeat. Thus, to assess whether the calcium-binding site of the annexin repeat sequence was involved in chemoresistance, another deletion mutant, R1(E70A) was constructed. Within the annexin repeat next to the N-terminal region, the 70th amino acid, glutamic acid, was responsible for the calcium-dependent activity of ANXA4 [30]. Accordingly, at this site, the point mutation variant of R1, R1(E70A), loses the function of its calcium-binding site (Fig. 4A). Similar to other deletion mutants, R1(E70A) was transfected into NUGC3 cells and designated R1(E70A)-95. Western blotting revealed that R1-12 had the same molecular weight as R1(E70A)-95 (Fig. 4B). R1(E70A)-95 did not induce resistance to either cisplatin or carboplatin (Fig. 4C). Moreover, the intracellular platinum content of R1(E70A)-95-transfected cells did not decrease compared with that of NC-14 cells after 0 hr

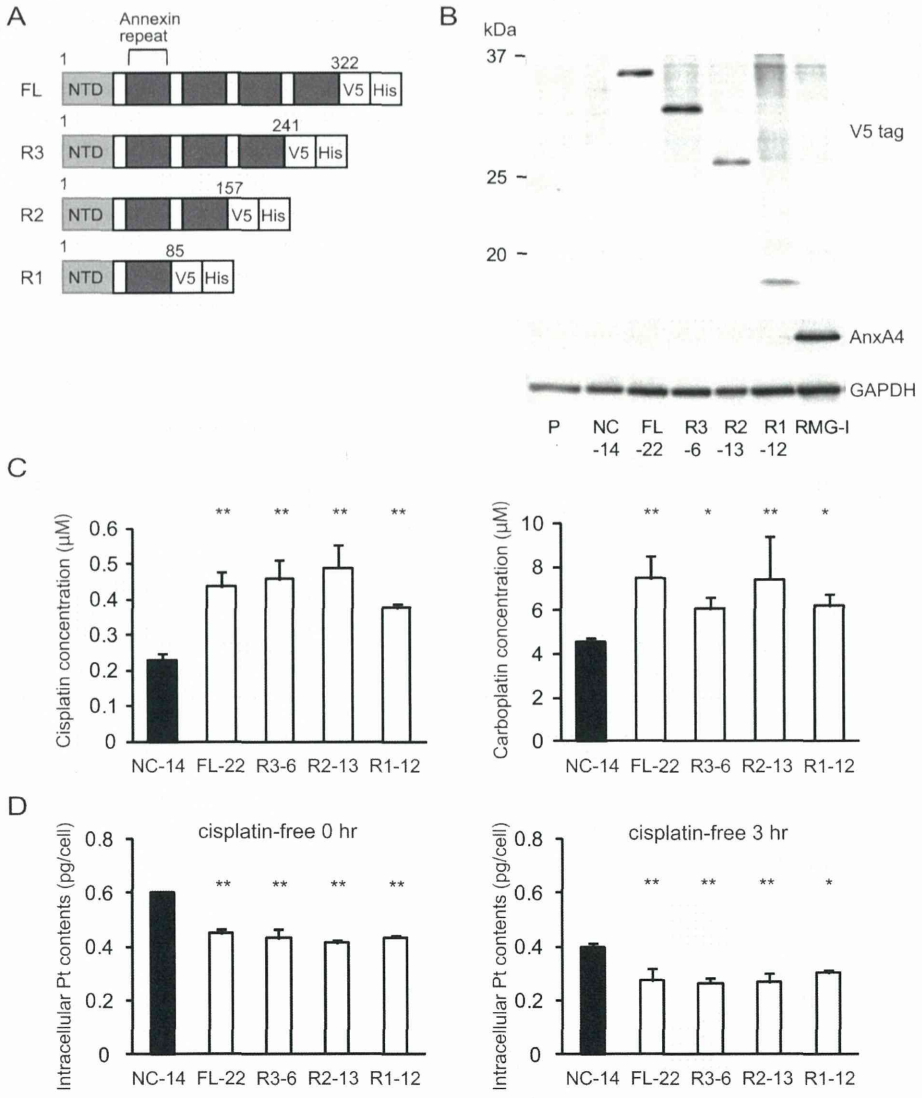

Fig.3: Annexin repeat domain is required for the platinum drug resistance. (A) A structural map of ANXA4 and 3 deletion mutant proteins. Annexin repeats were deleted one by one from the C-terminal site. (B) Established deletion mutant cells together with parent cells, control cells and RMG-I as a positive control were confirmed using Western blotting. (C) Compared with NC-14 cells, IC_{50} for both cisplatin and carboplatin was significantly increased in FL-22 and all other mutant cells. (D) Intracellular platinum accumulation after treatment with 100 μM cisplatin for 60 min with or without additional 3 hr of incubation in cisplatin-free medium. Data are presented as mean ± SD (*$p < 0.05$, **$p < 0.01$).